840 J. Med. Chem. 2010, 53, 840–849
DOI: 10.1021/jm901556u

Journal of Medicinal Chemistry Article

Cytotoxicity, Hydrophobicity, Uptake, and Distribution of Osmium(II) Anticancer Complexes in Ovarian Cancer Cells

Sabine H. van Rijt, Arindam Mukherjee, Ana M. Pizarro, and Peter J. Sadler*

Department of Chemistry, University of Warwick, Gibbet Hill Road, Coventry CV4 7AL, U.K.

Received October 20, 2009

The cytotoxicity, hydrophobicity (log *P*), cellular uptake, aqueous reactivity, and extent of DNA adduct formation in the A2780 ovarian carcinoma cells for four osmium(II) arene complexes [(η^6-arene)Os(4-methyl-picolinate)Cl] that differ only in their arene ligands as benzene (**1**), *p*-cymene (**2**), biphenyl (**3**), or tetrahydroanthracene (**4**) are reported. There is a correlation between hydrophobicity (log *P*), cellular uptake, nucleus uptake, and cytotoxicity of the complexes, following the order **3** ∼ **4** > **2** > **1**, suggesting that the arene plays an important role in the biological activity of these types of compounds. Cell distribution studies using fractionation showed that all four compounds distribute similarly within cells. DNA binding of osmium did not correlate with cytotoxicity, indicating that the nature of the DNA lesion may also be crucial to activity. TEM images of ovarian cells treated with **3** revealed morphological changes associated with apoptosis with possible involvement of mitochondria.

Introduction

Anticancer agents usually exert their therapeutic effect by their interaction with intracellular targets. However, the limited penetration of cytotoxic drugs into tumors is believed to be a major contributing factor to the frequent failure of chemotherapy to completely eradicate tumors in the clinic.[1] For example, in mice, the anticancer drug doxorubicin only diffuses 40−100 μm from blood vessels and shows limited penetration into the solid tumors.[2] The metal-based chemotherapeutic cisplatin is taken up into cells via active transport involving the copper transporter CTR1.[3,4] Unfortunately, cisplatin is also exported out of the cell via active transport involving multidrug-resistant proteins (MRP2 and possibly MRP3), as well as the copper transporters (ATP7B and possibly ATP7A).[5,6] Reduced uptake resulting from either increased efflux or reduced influx contributes toward acquired resistance of tumors with cisplatin.[7−9] An effective anticancer drug must reach all of the viable cells in a tumor and be retained in sufficient concentrations and on a relevant time scale to inhibit its intracellular target and initiate cell death.

Anticancer drugs based on other transition metals may address the problems associated with the platinum cytotoxics currently used in the clinic. A number of metal-based compounds with promising antiproliferative activity toward a wide range of tumors with novel mechanisms of action have recently been described.[10−16] The anticancer potential of the third-row transition metal osmium has only recently been explored. Osmium complexes have a reputation for being either toxic (OsO_4) or substitution-inert (many Os^{II} and Os^{III} complexes), perhaps explaining why their therapeutic potential has been little investigated. Encouragingly, certain classes of organometallic Os^{II} arene complexes appear to have promising in vitro cancer cell activity and their aqueous reactivity appears to be tunable.[17−22] In addition, some of these osmium complexes are non-cross-resistant with cisplatin toward cancer cells,[20,22] suggesting that they have a different mechanism of action and show potential for addressing the problem of intrinsic or acquired resistance in chemotherapy.

Here we have studied four osmium(II) arene complexes [(η^6-arene)Os(4-methyl-picolinate)Cl] that differ only in their η^6-coordinated arene ligand: benzene (**1**), *p*-cymene (**2**), biphenyl (**3**), and tetrahydroanthracene (**4**) (Figure 1). We have sought to correlate their differences in aqueous reactivity and hydrophobicity with their cytotoxicity, cellular uptake, DNA binding, and osmium distribution in cell fractions. In addition, a TEM[a] imaging study on complex **3** allowed observation of the distribution of osmium in ovarian cancer cells and provided insight into potential intracellular targets. This report is the first detailed study of cell uptake of anticancer Os^{II} arene complexes and reveals the importance of mitochondria as possible targets.

Results

Synthesis and Characterization. Osmium arene compounds **1**−**4** were prepared via their respective Cl-bridged dimers, [(η^6-arene)$OsCl_2$]$_2$, where arene = benzene (bz), *p*-cymene (*p*-cym), biphenyl (bip), and tetrahydroanthracene (THA), using previously reported methods.[23,24] The compounds were purified by crystallization from methanol and characterized by ^{1}H NMR spectroscopy, ESI-MS, and elemental analysis (see Supporting Information for details).

*To whom correspondence should be addressed. Phone: (+44) 024 7652 3818. Fax: (+44) 024 76523819. E-mail: p.j.sadler@warwick.ac.uk.

[a]Abbreviations: TEM, transmission electron microscopy; ESI-MS, electrospray ionization mass spectrometry; IC_{50}, half-maximum inhibitory concentration; ICP-MS, inductively coupled plasma mass spectrometry.

 Published on Web 12/15/2009

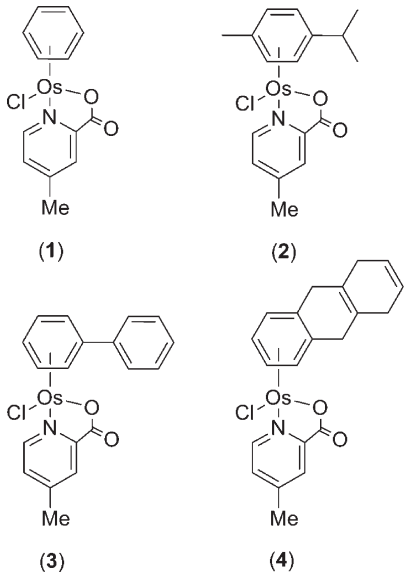

Figure 1. Chemical structures of the organometallic osmium(II) arene complexes studied in this work.

Table 1. In Vitro Growth Inhibition of A2780 Cells for Compounds **1**−**4** and Cisplatin (CDDP) as Control

compd	IC_{50} (μM)[a]
1	32.7 ± 0.8
2	7.6 ± 0.3
3	3.2[b]
4	4.5 ± 0.1
CDDP	2.2 ± 0.1

[a] Drug-treatment period was 24 h. Each value represents the mean ± SD for three independent experiments. [b] From ref 20.

In Vitro Growth Inhibition. All four complexes **1**, **2**, **3**, and **4** (Figure 1) exhibit activity in the A2780 ovarian cancer cell line with IC_{50} values of 3−33 μM (Table 1). The IC_{50} value for complex **3** is from our recent report (IC_{50} = 3.2 μM, under the same conditions).[20] Potency follows the order **4** ∼ **3** > **2** ≫ **1**. The least active is the benzene complex. The extended arene derivatives have IC_{50} values of 3−7 μM, comparable to that of drug carboplatin using a similar protocol (IC_{50} = 6 μM).

Hydrophobicity (log *P*). To assess a possible correlation between the biological activity and hydrophobicity of the osmium arene complexes, the partition coefficients (log *P*) in an octanol−water system were determined (Figure 2). Doubly distilled water containing 300 mM sodium chloride was used in order to suppress hydrolysis of the compounds, ensuring the determination of the log *P* of the chlorido complexes. The log *P* values increase in the order **1** < **2** < **4** < **3** with −0.51 ± 0.12 for **1**, 0.22 ± 0.04 for **2**, 0.71 ± 0.22 for **4**, and 0.86 ± 0.02 for **3**. These log *P* values are as expected; hydrophobicity increases with increasing size of the arene ligand. However, the two-ring system, bip, showed a slightly higher log *P* value than the three-ring system, with THA as the arene ligand. Only complex **1**, containing the benzene arene ligand, has a negative log *P* value (partitions preferentially into water, Figure 2).

Aqueous Reactivity. One possible route for in vivo activation of complexes of the type [(η^6-arene)M(XY)Cl], where M is Os^{II} or Ru^{II}, and XY is a chelating ligand, involves aquation (replacement of Cl by H_2O), since Os−OH_2 bonds are often more reactive than Os−Cl bonds. This may be the rate-limiting step in reactions with targets such as DNA.[25]

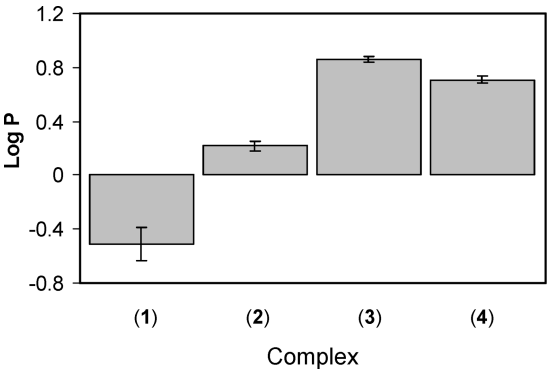

Figure 2. The log *P* values for complexes **1**−**4**. Results are the mean of six independent experiments and are expressed as mean ± SD.

Table 2. Hydrolysis Data for Compounds **1**−**4**

compd	k', h^{-1} [a]	$t_{1/2}$, h
1	1.63 ± 0.14	0.42 ± 0.04
2	1.80 ± 0.16	0.39 ± 0.04
3	0.71 ± 0.01[b]	0.98 ± 0.02[b]
4	1.36 ± 0.17	0.51 ± 0.07

[a] k' is the pseudo-first-order rate constant determined for hydrolysis of 0.8 mM **1**−**4** in deionized water at 288 K by ^{1}H NMR. [b] From ref 20.

To investigate the aqueous reactivity of these complexes, the rates of hydrolysis of compounds **1**, **2**, and **4** in a 5% MeOD-d_4/95% D_2O were monitored by ^{1}H NMR at 288 K by the observation of new peaks over time due to aqua adduct formation. The half-life of compound **3** has recently been reported to be $t_{1/2}$ = 0.98 ± 0.02 h under the same conditions.[20] The percentage of aqua peak formation for **1**, **2**, and **4** was plotted against time and was fitted to pseudo-first-order kinetics (Figure S1), and their half-lives were calculated (Table 2). Compounds **1**, **2**, and **4** hydrolyzed with half-lives ranging from 0.39 to 0.51 h. The extent of hydrolysis at equilibrium was 100% for **1**, 80% for **2**, and 60% for **4** (Figure S1) and was previously reported to be 96% for **3**.[20] The hydrolysis rate determined for compound **1** is a true pseudo-first-order rate since complete hydrolysis was observed, while for the other compounds the rate represents the pseudo-first-order rate for the approach to equilibrium since hydrolysis was incomplete.

The effects of chloride concentrations typical of those of blood plasma (100 mM), cell cytoplasm (22.7 mM), and cell nucleus (4 mM) on the aqueous equilibrium of compounds **1**, **2**, and **4** were investigated. ^{1}H NMR spectra of the compounds (1 mM) were recorded after enough time had been left for equilibration (at least four times their respective half-lives). These same experiments have previously been reported for compound **3**.[20]

Compound **1** was present 100% as its aqua species at 4 mM and 22.7 mM NaCl concentrations; at 100 mM NaCl, 47% was present as the aqua adduct. For compounds **2**, **3**, and **4**, at the low NaCl concentration of 4 mM, 56% (**2**), 81% (**3**), and 67% (**4**) were hydrolyzed, at 22.7 mM NaCl, 44% (**2**), 53% (**3**), and 50% (**4**) were hydrolyzed, and at 100 mM NaCl, 2% (**2**), 20% (**3**), and 0% (**4**) were hydrolyzed (Table 3); i.e., hydrolysis is likely to be almost completely suppressed for complexes **2**, **3**, and **4** in extracellular media.

Table 3. Percentage of Aqua Adduct Formation in an Equilibrated Solution of 1 mM **1**−**4** in D_2O at Chloride Levels Typical of Blood Plasma (100 mM), Cell Cytoplasm (22.7 mM), and Cell Nucleus (4 mM)

	% aqua adduct		
compd	4 mM NaCl	22.7 mM NaCl	100 mM NaCl
1	100	100	47
2	56	44	2
3	81[a]	53[a]	20[a]
4	67	50	0

[a] From ref 20.

Table 4. Cellular and DNA Osmium Concentrations in A2780 Ovarian Cells[a]

	cellular uptake (pmol Os/10^6 cells)		DNA binding (pmol Os/10^6 cells)	
Os complex	mean	SD	mean	SD
1	26.2	3.3	0.9	0.2
2	59.2	13.4	0.6	0.3
3	94.1	8.2	1.3	0.3
4	99.1	9.3	4.9	0.9

[a] Drug-treatment period was 24 h with 5 μM Os arene complexes. Each value represents the mean ± SD for six independent experiments.

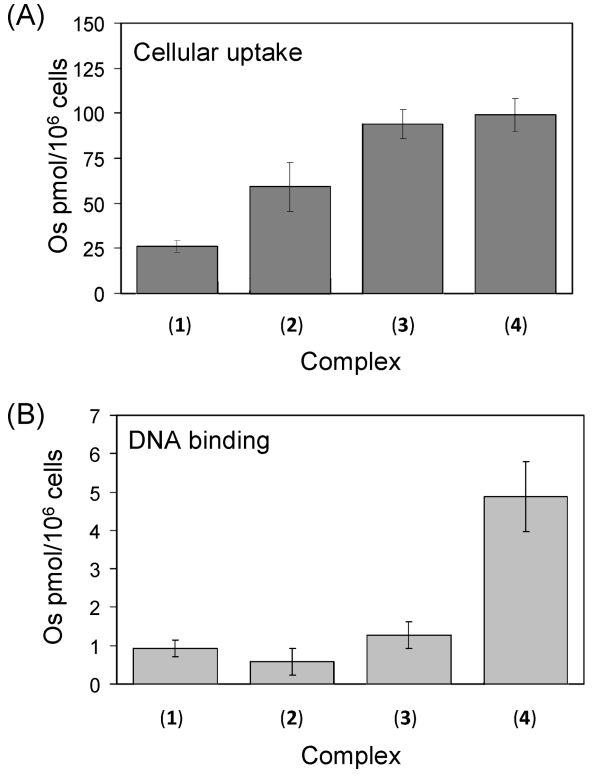

Figure 3. Osmium concentrations determined in A2780 cells after 24 h of exposure to 5 μM complexes **1**−**4** in (A) whole cells and (B) isolated DNA. Results are the mean of six independent samples and are expressed as mean ± SD.

Uptake into A2780 Cells. The uptake of compounds **1**−**4** by the A2780 ovarian cancer cell line was studied to investigate a possible relationship between the cellular uptake, hydrophobicity, and in vitro cytotoxicity of the complexes. Both cellular and DNA osmium concentrations were determined after 24 h of exposure to the complexes at 5 μM, which is an average of the IC_{50} values of complexes **2**−**4**. The results are summarized in Table 4 and Figure 3A. The highest

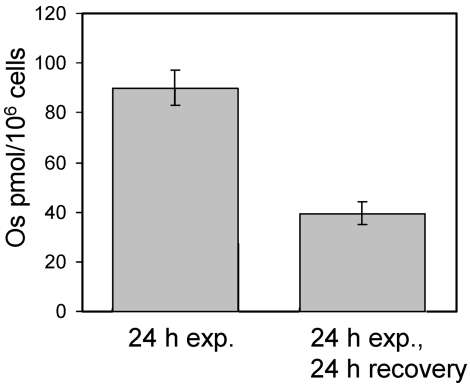

Figure 4. Cellular osmium concentrations determined in A2780 cells after exposure to 5 μM complex **3** for 24 h followed by 24 h in drug-free medium. Results are the mean of three independent experiments and are expressed as mean ± SD.

intracellular levels of osmium were observed after exposure to complexes **4** (99 ± 9 pmol Os/10^6 cells) and **3** (94 ± 8 pmol Os/10^6 cells), followed by complexes **2** and **1**, with levels of 59 ± 13 pmol Os/10^6 cells and 26 ± 3 pmol Os/10^6 cells, respectively.

For complex **3**, the cellular uptake after 24 h of exposure followed by a 24 h recovery period in drug-free medium was determined (Figure 4). At the end of the 24 h drug exposure, the cellular uptake was consistent with previous experiments. One day after the drug removal, the amount of osmium taken up by the cells had decreased by about 55% (from 90 ± 7 pmol Os/10^6 cells to 40 ± 4 pmol Os/10^6 cells, Figure 4).

The cellular uptake in A2780 cells for complex **3** as a function of time (t = 1, 2, 4, 8, 12, 24, and 48 h) was investigated (Figure 5). The maximum cell uptake was reached after 12 h of exposure (97 ± 5 pmol Os/10^6 cells). After 24 and 48 h of exposure to **3**, the amount of osmium decreased to 86 ± 12 pmol Os/10^6 cells and 71 ± 10 pmol Os/10^6 cells, respectively (Figure 5A). For the first 8 h of exposure to **3**, the cell count was still increasing. However, after 12 and 24 h of exposure, the cell count decreased and after 48 h about 80% fewer cells were counted compared to those present after 12 h of exposure (Figure 5B).

DNA Adduct Formation. As for chemotherapeutic cisplatin, DNA is believed to be the main target for this type of osmium arene complexes.[26] For this reason, DNA from A2780 cells was isolated and the levels of osmium on DNA were determined. The concentrations of osmium on the DNA follow a trend different from that observed for cellular uptake. Compound **4** shows the highest level of osmium on DNA (4.9 ± 0.9 pmol Os/10^6 cells) followed by compounds **3**, **1**, and **2** (1.3 ± 0.3, 0.9 ± 0.2, and 0.6 ± 0.3 pmol Os/10^6 cells, respectively) (Figure 3B). These values correspond to 1.0−4.9% of osmium−DNA adduct formation compared to the total amount of osmium that was taken up by the whole cell (i.e., 4.9% for **4**, 1.4% for **3**, 3.4% for **1**, and 1.0% for **2**).

Distribution of Osmium in Cell Fractions. The osmium content in nuclei, cytosol, and membrane fractions isolated from A2780 cells after 24 h of exposure to complexes **1**−**4** was determined, and the results are shown in Table 5 and Figure 6. The total amounts of osmium in the nuclear and cytosolic cell fractions follow the same trend as was observed for whole-cell uptake; the total amount of osmium in the fractions decreases in the order **3** ∼ **4** > **2** > **1**. For all four

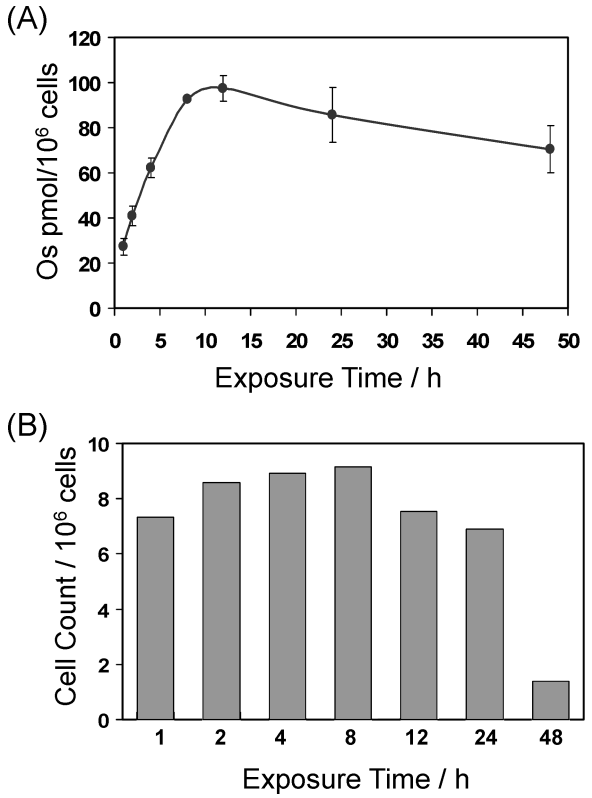

Figure 5. (A) Cellular osmium concentrations determined in A2780 cells after 1, 2, 4, 8, 12, 24, and 48 h exposure to 5 μM complex **3** and (B) cell counts for the different time points. Results are the mean of three independent samples and are expressed as mean ± SD.

Table 5. Nucleus, Cytosol, and Membrane/Cytoskeleton Osmium Concentrations in A2780 Ovarian Cells[a]

	uptake (pmol Os/10^6 cells)					
	cytosol		nucleus		membrane and cytoskeleton retention	
Os complex	mean	SD	mean	SD	mean	SD
1	12.6	2.3	2.3	0.4	1.8	0.1
2	31.1	6.6	4.7	0.9	7.5	0.9
3	38.6	3.8	10.5	0.9	11.3	0.7
4	46.9	5.1	8.4	1.0	4.4	0.9

[a] Drug-treatment period was 24 h with 5 μM Os arene complexes. Each value represents the mean ± SD for six independent experiments.

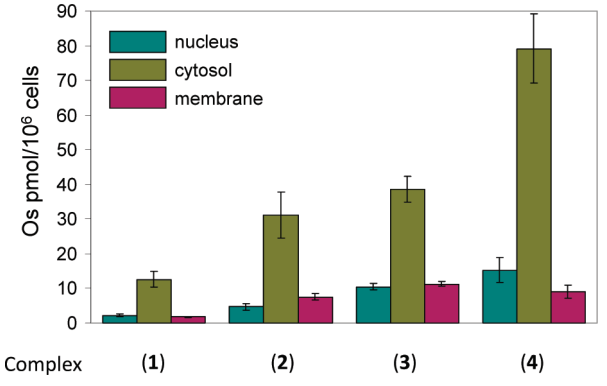

Figure 6. Osmium concentration in nucleus, cytosol, and membrane fractions (pmol Os/10^6 cells) in A2780 ovarian cells after 24 h of exposure to 5 μM **1**−**4**. Results are the mean of six independent experiments and are expressed as mean ± SD.

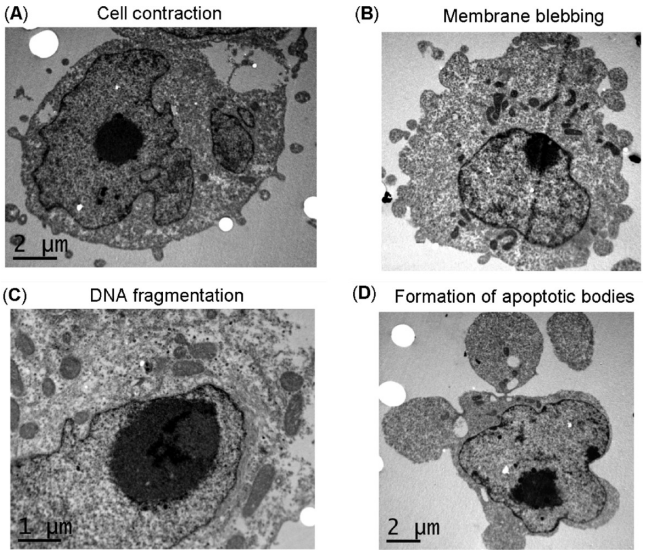

Figure 7. TEM images of A2780 cells exposed to complex **3**, showing the different stages of cell apoptosis: (A) cell contraction; (B) membrane blebbing; (C) DNA fragmentation; (D) the formation of apoptotic bodies.

complexes, the amount of osmium detected accounted for about 58−66% of the total osmium taken up by the cells (Table 5). This can be attributed to the loss of osmium during the fraction-separation procedures. The distribution of osmium observed for the Os^{II} compounds in the nuclear and cytosolic fractions is very similar for all four complexes; with 14% (**1**), 11% (**2**), 17% (**3**) and 14% (**4**) of the total amount of osmium in the fractions localizing in the cell nucleus and with 76% (**1**), 72% (**2**), 64% (**3**), and 79% (**4**) of osmium found in the cytosolic fractions.

Osmium was also found in the cell membrane/cytoskeleton fractions, with especially high values for complexes **2** and **3** of 7.5 ± 0.9 pmol Os/10^6 cells (17%) for **2**, and 11.3 ± 0.9 pmol Os/10^6 cells (19%) for **3**, respectively (Table 5, Figure 6).

Distribution of Osmium Using Transmission Electron Microscopy (TEM). The high electron density of osmium is frequently exploited for staining biological samples in various forms of electron microscopy. In particular, OsO_4 is a widely used staining agent in TEM and provides contrast to the image. It seemed likely that we would observe osmium-derived contrast in sections of cancer cells treated with the complexes studied here if their deposition is sufficiently localized in cell organelles.

A2780 cells were exposed to 5 or 20 μM biphenyl complex **3** for 12 h, and the treated and control cells were fixed and embedded in Epon resin. Ultrathin sections were observed under the TEM (Figures 7−10 and Figures S2−S4). The control cells and the treated cells were stained only with 2% uranyl acetate. Any additional contrast observed between the control cells and the treated cells is due to cell uptake of complex **3**.

In the cells exposed to complex **3**, morphological changes associated with cell apoptosis were identified: cell contraction (Figure 7A, Figure S2A,B), cell membrane blebbing (Figure 7B, Figure S2C,D), DNA fragmentation (Figure 7C, Figure S2E,F), and the formation of apoptotic bodies (Figure 7D, Figure S3).

In the control cells, the nucleus and mitochondria can be observed with relatively little contrast. The control cells do

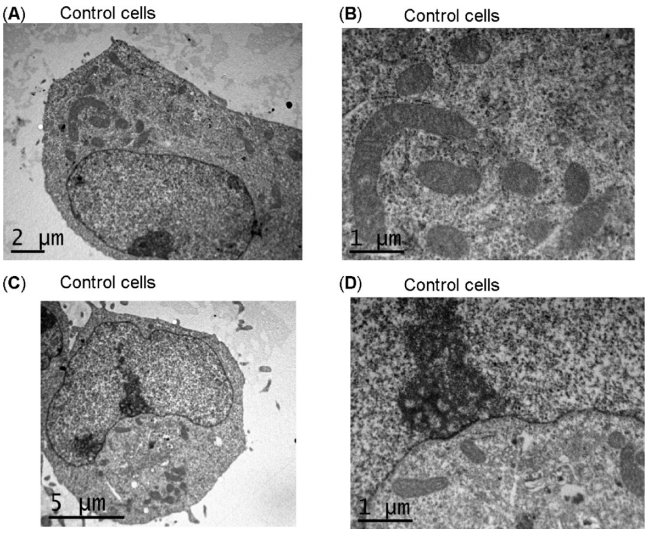

Figure 8. (A−D) TEM images of A2780 untreated control cells where (B) and (D) are magnifications of (A) and (B), respectively.

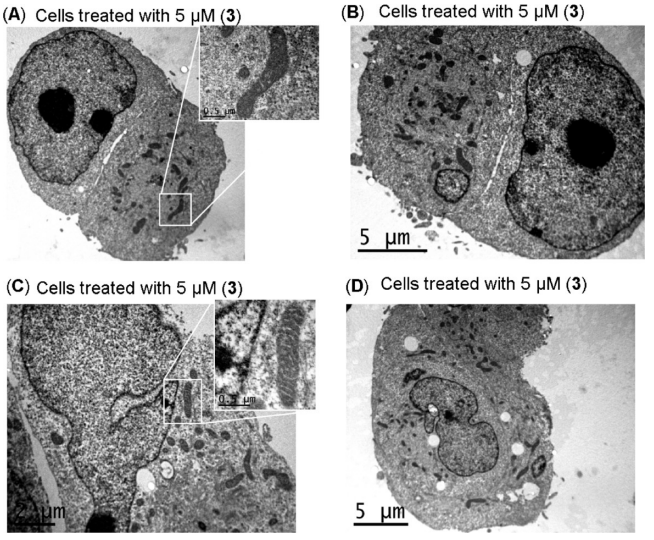

Figure 9. (A−D) TEM images of A2780 cells after 12 h of exposure to 5 μM complex **3**. Osmium complex **3** accumulates mainly in the mitochondria, nucleolus, and nuclear membrane. The insets in (A) and (C) show magnifications.

not appear to be distressed, and the cell membranes are intact (Figure 8 and Figure S4).

Sections of cells treated with 5 μM complex **3** show more contrast in comparison to those from control cells, in particular in the mitochondria, nucleolus, and the nuclear membrane (Figure 9, Figure S5). Several cells displayed the morphological changes associated with apoptosis. Some cell sections appear nonstressed and just display more contrast compared to the control cells (Figure 9A,B). Other cells appear distressed showing nuclear and cellular membranes with abnormal appearances (Figure 9C,D and Figure S5).

Cells treated with 20 μM complex **3** appear much more distressed than the cells treated with 5 μM **3**, as demonstrated by abnormal-looking cell and nuclear membranes for all cells (Figure 10A−D and Figure S6A−C). Many of the cells appear to be undergoing apoptosis. Also, these cells display even more contrast compared to the control cells and the cells treated with 5 μM **3**. In particular, the osmium complex

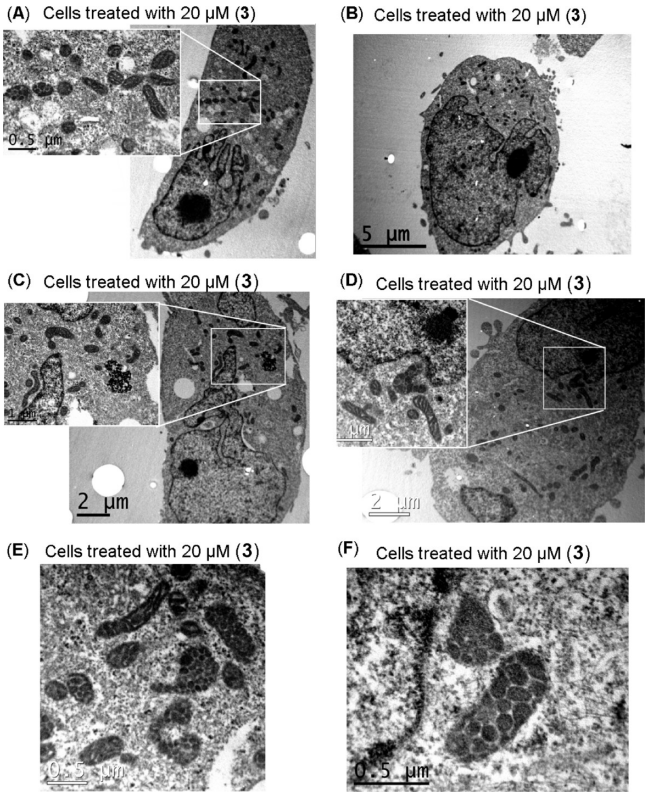

Figure 10. (A−F) TEM images of A2780 cells after 12 h of exposure to 20 μM complex **3**. Osmium complex **3** accumulates mainly in the mitochondria, nucleolus, and nuclear membrane. Also, swelling and different morphology of the mitochondria are observed (D, inset, E, and F). The insets in (A), (C), and (D) show magnifications.

appears to accumulate in the mitochondria, and swelling of the mitochondria seems to occur. In addition, some mitochondria show different morphology with circular cristae instead of the lamella-like structures observed in some of the other mitochondria (Figure 10D−F and Figure S6D−F).

Discussion

In this work we have investigated possible relationships between the hydrophobicity, cellular uptake, and cytotoxicity in the A2780 ovarian cancer cell line of four organometallic osmium(II) complexes [(η^6-arene)Os(4-methyl-picolinate)Cl] which have different arene ligands, ranging from a single benzene ring (**1**), *p*-cymene (**2**), to the two phenyl rings of biphenyl (**3**) and three fused rings of tetrahydroanthracene (**4**). In addition, time-dependent cell uptake, the distribution of osmium in cell fractions, DNA binding, and TEM imaging of cell sections were studied to gain insight into the mechanism of action of these osmium arene complexes.

Hydrophobicity, Cancer Cell Activity, and Cell Uptake. The log *P* value is a measure for hydrophobicity and has been investigated as a factor relevant to anticancer activity of metal-based drugs for many years. For several classes of metalloanticancer complexes a correlation between increased hydrophobicity and increased cytotoxic activity has been reported.[9,27−29] Several studies report on Pt^{II} and Pt^{IV} compounds, relating hydrophobicity with cell uptake.[30−32]

In this study, the hydrophobicity, cancer cell activity, and cell uptake correlated significantly, following the order **4** ∼ **3** > **2** > **1**. Compound **1** was the least hydrophobic, the least

cytotoxic, and the least taken up by the cells, whereas compounds **4** and **3** displayed the highest hydrophobicity, were the most cytotoxic, and were the most taken up by the cells. These data suggest that in the ovarian A2780 cancer cell line, the log *P* value can be used to predict the cytotoxicity for this class of osmium compound. These data also show that using more extended coordinated arenes such as biphenyl and tetrahydroanthracene results in increased hydrophobicity leading to higher cellular uptake and higher cytotoxicity. In addition, it is likely that the coordinated arenes are also involved in interactions with potential biological targets. The significantly lower cytotoxicity of the unsubstituted arene (benzene) compound **1** compared to the substituted arene complexes **2**−**4** indicates that the substituents on the arene in these complexes do play a part in the mechanism of their cytotoxicity. This could be rationalized in part, for example, by the intercalation of the extended arenes in **3** and **4** between DNA bases when the complexes bind to the major groove of DNA, as is also observed for the analogous ruthenium(II) complexes.[33,34] In the case of complex **2**, the arene (*p*-cymene) may perturb DNA structure in the major groove via steric interactions (i.e., upon binding of **2** to a nucleobase, the methyl and isopropyl substituents on the arene ring may cause additional distortions to the structure of DNA).

Time-dependent cell uptake experiments with complex **3** showed that the maximum cell uptake is reached after 12 h, after which time a decrease in osmium concentration and cell number is observed (Figure 5). This shows that the optimum time for induction of the death of A2780 ovarian cancer cells is between 12 and 48 h. A decrease in osmium concentration of about 55% after measuring the osmium content 24 h after the end of a 24 h exposure to **3** indicates that osmium efflux from the cells can occur.

Aqueous Reactivity. Improved understanding of the aqueous chemistry of organometallic complexes under biologically relevant conditions should aid the rational design of metal anticancer complexes.

The hydrolysis rates for compounds **1**, **2**, and **4** were measured by ^{1}H NMR at 288 K. All complexes hydrolyzed relatively rapidly with half-lives ($t_{1/2}$) between 0.39 and 0.98 h. There appears to be no link between the hydrolysis rates of these arene compounds and their biological activity. Furthermore, increasing the temperature to the biologically relevant temperature of 310K would increase the rate by about 8-fold.[18] This suggests that at 310 K, all four complexes would hydrolyze within a few minutes to form the reactive cationic aqua species in low-chloride intracellular compartments. However, at the higher chloride concentration of 100 mM (typical of blood plasma), compounds **2**−**4** are 80−100% present at equilibrium as the intact chloro ("prodrug") species. At a lower chloride concentration resembling that in the cell cytoplasm (22.7 mM), 44−53% of complexes **2**−**4** is present as the active hydrolyzed form, and at the lowest chloride concentration of 4 mM, close to that of the cell nucleus, complexes **2**−**4** are 56−81% present as the reactive aqua species (Table 3). These data indicate that in the cell nucleus, complexes **2**−**4** might be selectively activated through hydrolysis as a mode of activation toward DNA binding, while outside the cell and in particular in blood plasma, complexes **2**−**4** are predominately present as their less reactive intact chlorido species. From this it can be concluded that the complexes are taken up by cells predominately in their neutral chlorido forms, their cell uptake dominated by the hydrophobicity of the coordinated arenes, while in the cytoplasm, the complexes exist as equilibrium mixtures of their chlorido and aqua forms. The aqua species may react with proteins and organelles in the cytoplasm and, being positively charged and lipophilic, may target mitochondria. On the other hand, the chlorido species, being relatively unreactive, are able to cross the nuclear membrane and then hydrolyze and react with the negatively charged DNA.

Compound **1** exhibits a different behavior: at chloride concentrations of 4 and 22.7 mM, **1** is completely hydrolyzed, and at high NaCl concentrations of 100 mM about 50% is present in its chlorido "prodrug" form. The presence of the reactive aqua species of **1** at relatively high NaCl concentrations may partly explain the reduced cell uptake and more moderate cytotoxicity of this complex compared to **2**, **3**, and **4**. The reactive aqua adduct of **1** may be deactivated by biomolecules on its way to its target either in blood plasma or in the cytoplasm.

Distribution of the Osmium Complexes in Cell Fractions. The uptake of the four complexes into the different cell fractions follows the same trend as was observed for whole cell uptake (i.e., the total amount of osmium in the fractions follows the order **3** ∼ **4** > **2** > **1**). Importantly, there is a correlation between the nucleus uptake and cytotoxicity of the complexes, both of which follow the order **3** > **4** > **2** > **1**, suggesting that penetrating the nucleus and binding to nuclear DNA might make a major contribution to the mechanism of cytotoxicity. The distribution of the osmium over the several isolated cell fractions is very similar for all four osmium compounds; with 11−17% of the total of the osmium in the different fractions reaching the cell nucleus, 64−79% was found in the cytosolic fractions and also significant amounts of osmium were found in the outer cell membrane and cytoskeleton fractions, in particular for compounds **2** and **3** (Table 5, Figure 6). This indicates that once in the cell, the osmium complexes distribute over the cell independent of the nature of the arene or their hydrophobicity. Significant amounts of osmium reach the cell nucleus for all four compounds. In particular, 13% of the overall osmium uptake for compound **1** reaches the nucleus, displaying a similar distribution as complexes **2**−**4**. This is surprising because its aqueous chemistry is significantly different from that of **2**−**4**; the reactive aqua species forms even at relatively high chloride concentrations.

DNA Adduct Formation. Osmium(II) arene complexes are believed to interact with DNA in a similar manner as their ruthenium analogues, i.e., binding to N7 of guanine in combination with H-bonding (if there is a neighboring NH on an Os ligand) and noncovalent arene intercalation into DNA.[26] With the present data it is possible to examine whether there is a relationship between the extent of DNA binding and the cytotoxicity of the complexes.

The amount of osmium found on the DNA of A2780 cells follows the order; **4** ≫ **3** > **1** > **2** and does not correlate with cytotoxic potency or hydrophobicity (log *P*) or cellular uptake (Table 5, Figure 3). The extent of osmium binding of **1**−**4** to DNA, which amounts to 1.0−4.9% of the total osmium taken up by the cells, appears to be low. However, this is a similar level to that reported for cellular platination of DNA by cisplatin (∼1%).[35−37] Therefore, it is reasonable to assume that DNA is a potential target for these cytotoxic osmium complexes. Although complex **4** exhibits the highest level of DNA binding, it is not the most potent complex

(Table 1). These data suggest not only that it is important for osmium to reach the DNA but also that the nature of the lesion on DNA (including structural distortions) is an important factor in determining cytotoxic activity. However, we cannot rule out the possibility that nuclear DNA may not be the only target for these complexes.

Distribution of Osmium Using TEM. TEM images of ovarian cells exposed to complex **3** for 12 h show morphological changes to the cells that are commonly associated with cell apoptosis.[38] These include cell contraction (Figure 7A, Figure S2A,B), dynamic membrane blebbing (Figure 7B, Figure S2C,D), and DNA fragmentation (Figure 7C, Figure S2E,F). Also, the formation of apoptotic bodies was observed in several images, marking the final stage of cell apoptosis (Figure 7D, Figure S3). We can therefore conclude that osmium complex **3** and probably the other structurally similar osmium complexes induce cell death via apoptotic pathways rather than necrosis.

The micrographs from cells exposed to 5 μM complex **3** illustrate that **3** accumulates mainly in the mitochondria, nucleolus, and nuclear membrane (Figure 9 and Figure S5). Several images show apoptotic cells and some cells appear distressed, as evidenced by the abnormal looking nucleus and cellular membranes (Figure 9C,D and Figure S5). All cells exposed to 20 μM complex **3** (6.25 times its IC_{50} value) appeared distressed and/or apoptotic. Also, in these cells the accumulation of **3** in the mitochondria, nucleolus, and nuclear membrane becomes even more clearly visible (Figure 10A−D and Figure S6A−D). In particular the mitochondria are heavily stained and the internal structures of the mitochondria become clearly visible. In addition, the morphology of some of the mitochondria is very different from that observed for control cells and cells exposed to 5 μM **3**; condensed cristae and swelling are observed (Figure 10D−F and Figure S6D−F). The intensely dark-colored mitochondria suggest that osmium complex **3** accumulates inside the cristae as well as in the inner and outer membranes of the mitochondria. This suggests that mitochondria may be a target for these osmium arene complexes or that the swelling and morphological changes of the mitochondria arise as a consequence of apoptosis. Although little is known about the relationship between alterations in mitochondrial morphology and activation of the mitochondrial apoptotic pathway, a few studies have associated changes in mitochondrial morphology with apoptosis induced in cultured cells by different apoptotic stimuli. These changes have mainly been described as disorganization, condensation, or swelling.[39−43]

From the cell fractionation studies it was shown that about three-quarter to one-third of the osmium that is taken up by cells is present in the cytosolic fraction after 24 h of exposure to compounds **1**−**4**, indicating that the complexes may be interacting with organelles and biomolecules present in the cytosol. In addition, the osmium complexes appear to have affinity for the cellular membranes. This is demonstrated by the dark-colored nuclear membrane in the TEM images and by the cell fractionation studies, in which large amounts of osmium were detected in the membrane/cytoskeleton fractions, especially for complexes **2** and **3**. Mitochondria may represent potential targets, and the abundance of osmium in mitochondrial membranes may explain why so much osmium remains in the cytosol.

Other metal-based anticancer complexes known to target mitochondria include several gold(I) and gold(III) complexes that irreversibly inhibit mitochondrial human glutathione reductase (hGR) and thioredoxin reductase (hTrxR).[10,44] Another example is the structurally related Ru^{II} phosphine compound [Ru(η^6-*p*-cymene)Cl_2(pta)]. Its cytotoxicity is thought to be mediated by mitochondrial and JNK-p53 pathways.[45]

In previous work we have shown that osmium arene complexes related to those studied here can bind to several nucleobases, with a high affinity for guanine. We have shown that these complexes bind to calf thymus DNA and cause DNA unwinding (instead of DNA bending seen for ruthenium arene complexes).[18,20,26,46,47] Our results support the possibility that permeation of these osmium complexes into mitochondria and the cell nucleus may be followed by their binding to and distortion of the mitochondrial or nuclear DNA, leading to cell apoptosis which causes the morphological changes observed in the TEM images of cell sections. Although it cannot be confirmed whether binding of osmium to mitochondrial or nuclear DNA is the major pathway to apoptosis, the images of cell sections provide the first evidence that mitochondria may be involved for these and related osmium arene complexes.

Conclusions

This study shows that the hydrophobicity (log *P*), cancer cell activity, and cell uptake for four osmium arene complexes are significantly correlated. This suggests that log *P* values may be useful indicators of A2780 cancer cell cytotoxicity for this class of Os^{II} arene complexes. Furthermore, this work shows that the arene ligand plays an important part in the cytotoxicity; the presence of substituted arenes not only resulted in higher hydrophobicity and increased uptake by the cell but also seemed to play an important part in the mechanism of cytotoxicity of the complexes.

From the TEM images and from the cell fractionation studies it appears that the osmium compounds accumulate in cellular, mitochondrial, and nuclear membranes in significant amounts. The TEM images of cell sections also revealed morphological changes associated with apoptosis in A2780 cells exposed to [(η^6-biphenyl)Os(4-methylpicolinate)Cl] (**3**) excluding necrosis as possible cause for cell death for this complex and likely for structurally similar osmium complexes.

There is a correlation between nucleus uptake and cytotoxicity of the compounds, suggesting that nucleus uptake and binding to nuclear DNA may be the major pathway for cytotoxicity. However, the levels of osmium binding to DNA were relatively low and do not correlate with cytotoxic potency. This in combination with the mitochondrial swelling and morphology changes observed by TEM imaging suggests that the nature of the DNA lesion may be of importance and also raises the possibility that mitochondrial apoptotic pathways are involved.

Experimental Section

Materials. 1,4-Dihydrobiphenyl and the dimers [(η^6-*p*-cym)$OsCl_2]_2$, [(η^6-bip)$OsCl_2]_2$, [(η^6-bz)$OsCl_2]_2$, and [(η^6-THA)$OsCl_2]_2$ were prepared using previously reported procedures.[23,24] $OsCl_3 \cdot nH_2O$ was purchased from Alfa Aesar. All deuterated solvents and cisplatin were obtained from Sigma Aldrich. Methanol was distilled over magnesium/iodine prior to use. Complexes **1**−**4** were synthesized from the dimeric precursors [(η^6-*p*-cym)$OsCl_2]_2$, [(η^6-bip)$OsCl_2]_2$, [(η^6-bz)$OsCl_2]_2$, and

$[(\eta^6\text{-THA})OsCl_2]_2$ using procedures similar to those reported previously for other half-sandwich Os^{II} arene complexes.[48,49] The 4-methylpicolinic acid ligand and complex **3**, $[(\eta^6\text{-bip})$Os-(4-methyl-picolinate)Cl], were synthesized and characterized as previously described.[20] The purities of compounds **1**, **2**, and **4** were all determined to be ≥95% by elemental analysis and are reported in the Supporting Information. In addition, ^{1}H NMR and ESI-MS data for compounds **1**, **2**, and **4** can also be found in the Supporting Information.

Preparation of the Complexes. [(η^6-Benzene)Os(4-methyl-picolinate)Cl] (1). A solution of $[(\eta^6\text{-bz})OsCl_2]_2$ (75 mg, 0.11 mmol) in dry and degassed MeOH (10 mL) was refluxed under argon for 1 h before adding a solution of sodium methoxide (2.2 mol equiv, 13 mg) and 4-methyl-picolinic acid (2.2 mol equiv, 39 mg) in 5 mL of dry and degassed MeOH. The resulting mixture was left to reflux mildly for 16 h, at which time a crystalline brown precipitate had formed. The brown powder was recovered by filtration and was air-dried to give a final yield of 30.7 mg (32%).

[(η^6-*p*-Cymene)Os(4-methyl-picolinate)Cl] (2). A solution of $[(\eta^6\text{-}p\text{-cym})OsCl_2]_2$ (70 mg, 0.103 mmol) in dry and degassed MeOH (10 mL) was refluxed under argon for 1 h before adding a solution of sodium methoxide (2.6 mol equiv, 14.5 mg) and 4-methyl-picolinic acid (2.6 mol equiv, 36.7 mg) in 5 mL of dry and degassed MeOH. The resulting mixture was left to reflux mildly for 3 h and was filtered, and the solvent was reduced on a rotary evaporator until a precipitate began to form and was left standing at 278 K. The yellow powder was recovered by filtration and was air-dried to give a final yield of 46.8 mg (46%).

[(η^6-Tetrahydroanthracene)Os(4-methyl-picolinate)Cl] (4). Synthesis was as for **2** using $[(\eta^6\text{-THA})OsCl_2]_2$ (67 mg, 0.076 mmol), sodium methoxide (2.6 mol equiv, 29 mg), and 4-methyl-picolinic acid (2.6 mol equiv, 10 mg). Yield: 25.6 mg (31%).

Instrumentation and Methods. Nuclear Magnetic Resonance (NMR) Spectroscopy. ^{1}H NMR spectra were acquired in 5 mm NMR tubes at 298 K (unless stated otherwise) on a Bruker DMX 500 (^{1}H = 500.13 MHz) spectrometer. ^{1}H NMR chemical shifts were internally referenced to $(CHD_2)(CD_3)SO$ (2.50 ppm) for DMSO-d_6 and to CHD_2OD (3.34 ppm) for methanol-d_4.

Elemental Analysis. Carbon, hydrogen, and nitrogen (CHN) elemental analyses were carried out on a CE-440 elemental analyzer by Exeter Analytical (UK) Ltd.

ICP-MS Instrumentation and Calibration. All ICP-MS analyses were carried out on an Agilent Technologies 7500 series ICP-MS instrument. The settings for ICP-MS are listed in Table S1. The water used for ICP-MS analysis was doubly deionized (DDW) using a USF Elga UHQ water deionizer. The osmium Specpure plasma standard (Alfa Aesar, 1000 ppm in 5% HCl) was diluted with DDW to 20 ppm. The standards for calibration were freshly prepared by diluting this stock solution with 3% HNO_3 in DDW. The concentrations used were 100, 60, 20, 10, 5, 4, 2, 1, 0.4, and 0.1 ppb. With the instrumentation settings listed in Table S1, the detection limit was typically 9 ppt (for 10 standards), and sensitivity was 270 900 ^{189}Os ion counts for 100 ppb of Os standard in no gas mode.

ESI-MS. Electrospray ionization mass spectra were obtained either on a Bruker Esquire 2000 spectrometer or a Bruker MicroTOF spectrometer. Samples were prepared in either water or a methanol/water mixture, and the cone voltage and source temperature varied depending on the sample. Data were processed using DataAnalysis 3.3 (Bruker Daltonics).

Aqueous Reactivity. The kinetics of hydrolysis for complexes **1**−**4** were followed by ^{1}H NMR at different temperatures. For this, solutions of the complexes with a final concentration of 0.8 mM in 5% MeOD-d_4/95% D_2O (v/v) were prepared by dissolution of the complexes in MeOD-d_4 followed by rapid dilution using D_2O with a pH* (pH meter reading without correction for effects of D on glass electrode) of ∼2 (acidified with HNO_3) so that the aqua ligand was not deprotonated. ^{1}H NMR spectra were taken after various intervals using the presaturation method for water surpression. The rate of hydrolysis was determined by fitting plots of concentrations (determined from ^{1}H NMR peak integrals) versus time to a pseudo-first-order equation using ORIGIN, version 7.5 (Microcal Software Ltd.).

The effects of varying concentrations of chloride on the extent of hydrolysis of the complexes at equilibrium were investigated by preparing aqueous solutions of **1**−**4** (1 mM) in 100, 22.7, and 4 mM NaCl in D_2O, recording spectra after enough time was left for equilibration (at least 4 times their respective half-lives).

Cell Culture. The A2780 ovarian cell line was obtained from the ECACC (European Collection of Animal Cell Culture, Salisbury, U.K.). The cells were maintained in RPMI 1640 media which was supplemented with 10% fetal calf serum, 1% L-glutamine, and 1% penicillin/streptomycin. All cells were grown at 310 K in a humidified atmosphere containing 5% CO_2.

In Vitro Growth Inhibition Assay. After plating, human ovarian A2780 cancer cells were treated with Os^{II} complexes on day 3 at concentrations ranging from 0.1 to 100 μM. Solutions of the Os^{II} complexes were made up in 0.125% (v/v) DMSO to assist dissolution (0.03% final concentration of DMSO per well in the 96-well plate). Cells were exposed to the complexes for 24 h, washed, supplied with fresh medium, and allowed to grow for 3 doubling times (72 h), and then the protein content was measured (proportional to cell survival) using the sulforhodamine B (SRB) assay.[50]

Drug Uptake, DNA Adduct Formation, and Cell Fractionation. A2780 cells were plated at a density of 5×10^6 cells/100 mm Petri dish in 12 mL of culture medium on day 1 (three dishes were prepared per compound tested and three untreated control dishes in two independent separate experiments). On day 2 cells were exposed to the Os^{II} arene complexes. Stock solutions (0.5 mM) of osmium compounds were made up fresh in 5% DMSO and saline before being diluted in media to give a final concentration of 5 μM. After 24 h of drug exposure, the drug-containing medium was removed. The cells were washed with PBS and trypsinized, and the cell suspension was counted. One-third of the cells were centrifuged, washed with PBS, and stored at 253 K. Another third of the samples was used for DNA extraction using the Nucleon genomic DNA extraction kit (GE healthcare, Amersham, U.K.) (BACC-1 protocol) and the last third for cytosol, nucleus, membrane/cytoskeleton fractionation using a cell fractionation kit (Biovision, Mountain View, CA) (fractionPREP). All samples were stored at 253 K until ICP-MS analysis for osmium content.

For the time-dependent cell uptake experiments, A2780 cells were plated at a density of 5×10^6 cells/100 mm Petri dish in 12 mL of culture medium on day 1 (three dishes were prepared per time point and three untreated control dishes). On day 2, cells were exposed to complex **3** at 5 μM (prepared as stated previously) at 1, 2, 4, 8, 12, and 24 h time intervals. After the indicated exposure times, cells were trypsinized and the cell suspension was counted. The cells were centrifuged, washed with PBS, and stored at 253 K until ICP-MS analysis for osmium content.

To establish the osmium uptake after a 24 h exposure and 24 h after the end of the exposure to complex **3**, A2780 cells were plated at a density of 5×10^6 cells/100 mm Petri dish in 12 mL of culture medium on day 1 (three dishes were prepared for the 24 h exposure, three dishes for 24 h of exposure and 24 h of recovery in drug-free media, and three untreated control dishes). On day 2, cells were exposed to complex **3** at 5 μM, prepared as stated previously. After 24 h of exposure to **3**, cells were trypsinised and the cell suspension was counted. The cells were centrifuged, washed with PBS, and stored at 253 K until ICP-MS analysis for osmium content. For three dishes, the drug containing medium was removed, cells were washed with PBS, and fresh medium was supplied. After a 24 h recovery period, the medium was

removed, cells were washed with PBS and trypsinized, and the cell suspension was counted. The cells were centrifuged, washed with PBS, and stored at 253 K until ICP-MS analysis for osmium content.

ICP-MS Analysis. The whole cell pellets, DNA samples, and cytosol/nucleus/membrane fractionation samples were digested as described below. To the cell pellets 0.8 mL and to the extracts 0.4 mL of freshly distilled 72% HNO_3 were added, and the samples were transferred into Wheaton V-Vials (Sigma Aldrich). The vials were heated in an oven at 373 K for 16 h to fully digest the samples and allowed to cool, and then each sample was transferred to a Falcon tube. The vials were washed with doubly deionized water (DDW) and the samples diluted 10 times with DDW to obtain 7.2% HNO_3 sample solutions.

Determination of Partition Coefficient, log *P*. Octanol-saturated water (OSW) and water-saturated octanol (WSO) were prepared using analytical grade octanol (Sigma) and 0.3 M aqueous NaCl solution. Aliquots of stock solutions of osmium complexes in OSW were added to equal volumes of WSO and shaken in an IKA Vibrax VXC basic shaker for 4 h at 500 g/min after partition. The aqueous and octanol layers were carefully separated into test tubes for osmium analysis. Aqueous samples before and after partitioning were diluted with 3% HNO_3 to the appropriate range for analysis by ICP-MS calibrated with aqueous standards (Os, 1−100 ppb). These procedures were carried out at ambient temperature (~298 K). Partition coefficients of Os^{II} arene complexes were calculated using the equation $\log P_{oct} = \log([Os]_{oct}/[Os]_{aq})$.

TEM Sample Preparations. A2780 cells were plated at a density of 5×10^6 cells/100 mm Petri dish in 12 mL of culture medium (two dishes were prepared for exposure to compound **3** and two dishes for untreated control plates). After 24 h, untreated cells received fresh media while treated cells were exposed to complex **3** at 20 and 5 μM. Stock solutions (0.5 mM) of osmium compounds were made up fresh in 5% DMSO and saline before being diluted in media to give final concentrations of 20 and 5 μM. After 12 h of drug exposure, the medium was removed and the cells were washed with PBS. The cells were fixed with 2% gluteraldehyde (Agar Scientific, Cambridge, U.K.) in cacodylate buffer at pH 7.6 (Agar Scientific, Cambridge, U.K.) for 1 h at ambient temperature (agitating on a shaker). The plates were rinsed for 10 min with cacodylate buffer, and this was repeated five times. The cells were scraped with a cell scraper and transferred in 0.5 mL of buffer into a 0.5 mL Eppendorf tube. The samples were stained with 2% uranyl acetate in maleate buffer (Agar Scientific, Cambridge, U.K.) for 1 h at ambient temperature. Cells were then dehydrated in graded series of ethanol with a final change of 100% ethanol overnight. Prior to embedding, the cells were infiltrated with 100% propylene oxide for 1 h followed by a 1:1 mixture of propylene oxide and Embed 812 resin (Agar Scientific, Cambridge, U.K.) for 6 h. This was then replaced with several changes of 100% resin over an 18 h period before curing for 24 h at 333 K. Blocks were trimmed and sectioned on a Leica Ultracut E ultramicrotome (Leica Microsystems, Milton Keynes, U.K.), and 70−80 nm sections were collected on 400-mesh copper grids and stained with uranyl acetate. The sections were imaged on a JEOL 1200EXII TEM with a 1K Gatan camera.

Acknowledgment. We thank Dr. Carol Evered (University of Warwick, U.K.) for help with the preparation and sectioning of the TEM samples and Dr. Lijiang Song (University of Warwick, U.K.) for help with ICP-MS. This research was supported by the EC (Marie Curie Fellowship for A.M.), MRC (Grant G0701062), University of Warwick and Science City (ERDF/AWM). The authors also acknowledge their participation in the EU COST Action D39 which enabled them to exchange regularly the most recent ideas in the field of anticancer metallodrugs with several European colleagues.

Supporting Information Available: Spectroscopic data and ESI-MS and CHN analysis data for complexes **1**, **2**, and **4**; instrumental settings for ICP-MS (Table S1); time dependence for formation of the aqua complexes of **1**, **2**, and **4** (Figure S1); TEM images of A2780 cells exposed to complex **3**, showing the different stages of cell apoptosis (Figures S2 and S3); TEM images of A2780 cells only stained with 2% uranyl acetate (controls) (Figure S4); TEM images of A2780 cells exposed to 5 μM complex **3** (Figure S5); TEM images of A2780 cells exposed to 20 μM complex **3** (Figure S6). This material is available free of charge via the Internet at http://pubs.acs.org.

References

(1) Tredan, O.; Galmarini, C. M.; Patel, K.; Tannock, I. F. Drug resistance and the solid tumor microenvironment. *J. Natl. Cancer Inst.* **2007**, *99*, 1441–1454.
(2) Minchinton, A. I.; Tannock, I. F. Drug penetration in solid tumours. *Nat. Rev. Cancer* **2006**, *6*, 583–592.
(3) Ishida, S.; Lee, J.; Thiele, D. J.; Herskowitz, I. Uptake of the anticancer drug cisplatin mediated by the copper transporter Ctr1 in yeast and mammals. *Proc. Natl. Acad. Sci. U.S.A.* **2002**, *99*, 14298–14302.
(4) Wang, D.; Lippard, S. J. Cellular processing of platinum anticancer drugs. *Nat. Rev. Drug Discovery* **2005**, *4*, 307–320.
(5) Borst, P.; Evers, R.; Kool, M.; Wijnholds, J. A family of drug transporters: the multidrug resistance-associated proteins. *J. Natl. Cancer Inst.* **2000**, *92*, 1295–1302.
(6) Safaei, R.; Howell, S. B. Copper transporters regulate the cellular pharmacology and sensitivity to Pt drugs. *Crit. Rev. Oncol. Hematol.* **2005**, *53*, 13–23.
(7) Klein, A. V.; Hambley, T. W. Platinum drug distribution in cancer cells and tumors. *Chem. Rev.* **2009**, *109*, 4911–4920.
(8) Rabik, C. A.; Dolan, M. E. Molecular mechanisms of resistance and toxicity associated with platinating agents. *Cancer Treat. Rev.* **2007**, *33*, 9–23.
(9) Loh, S. Y.; Mistry, P.; Kelland, L. R.; Abel, G.; Harrap, K. R. Reduced drug accumulation as a major mechanism of acquired resistance to cisplatin in a human ovarian carcinoma cell line: circumvention studies using novel platinum (II) and (IV) ammine/amine complexes. *Br. J. Cancer* **1992**, *66*, 1109–1115.
(10) Berners-Price, S. J.; Filipovska, A. The design of gold-based, mitochondria-targeted chemotherapeutics. *Aust. J. Chem.* **2008**, *61*, 661–668.
(11) Dyson, P. J.; Sava, G. Metal-based antitumor drugs in the post genomic era. *Dalton Trans.* **2006**, 1929–1933.
(12) Jakupec, M. A.; Galanski, M.; Arion, V. B.; Hartinger, C. G.; Keppler, B. K. Antitumor metal compounds: more than theme and variations. *Dalton Trans.* **2008**, 183–194.
(13) Melchart, M.; Sadler, P. J. Ruthenium Arene Anticancer Complexes. In *Bioorganometallics*; Jaouen, G., Ed.; Wiley-VCH: Weinheim, Germany, 2006; pp 39−64.
(14) Reedijk, J. Metal−ligand exchange kinetics in platinum and ruthenium complexes. Significance for effectiveness as anticancer drugs. *Platinum Met. Rev.* **2008**, *52*, 2–11.
(15) Bruijnincx, P. C. A.; Sadler, P. J. New trends for metal complexes with anticancer activity. *Curr. Opin. Chem. Biol.* **2008**, *12*, 197–206.
(16) van Rijt, S. H.; Sadler, P. J. Current applications and future potential for bioinorganic chemistry in the development of anticancer drugs. *Drug Discovery Today* **2009**, *14*, 1089–1097.
(17) Dorcier, A.; Ang, W. H.; Bolano, S.; Gonsalvi, L.; Juillerat-Jeannerat, L.; Laurenczy, G.; Peruzzini, M.; Phillips, A. D.; Zanobini, F.; Dyson, P. J. In vitro evaluation of rhodium and osmium RAPTA analogues: the case for organometallic anticancer drugs not based on ruthenium. *Organometallics* **2006**, *25*, 4090–4096.
(18) Peacock, A. F. A.; Parsons, S.; Sadler, P. J. Tuning the hydrolytic aqueous chemistry of osmium arene complexes with N,O-chelating ligands to achieve cancer cell cytotoxicity. *J. Am. Chem. Soc.* **2007**, *129*, 3348–3357.
(19) Schmid, W. F.; John, R. O.; Arion, V. B.; Jakupec, M. A.; Keppler, B. K. Highly antiproliferative ruthenium(II) and osmium(II) arene complexes with paullone-derived ligands. *Organometallics* **2007**, *26*, 6643–6652.
(20) van Rijt, S. H.; Peacock, A. F. A.; Johnstone, R. D. L.; Parsons, S.; Sadler, P. J. Organometallic osmium(II) arene anticancer

complexes containing picolinate derivatives. *Inorg. Chem.* **2009**, *48*, 1753–1762.
(21) Peacock, A. F. A.; Sadler, P. J. Medicinal organometallic chemistry: designing metal arene complexes as anticancer agents. *Chem. Asian J.* **2008**, *3*, 1890–1899.
(22) van Rijt, S. H.; Hebden, A. J.; Amaresekera, T.; Deeth, R. J.; Clarkson, G. J.; Parsons, S.; McGowan, P. C.; Sadler, P. J. Amide linkage isomerism as an activity switch for organometallic osmium and ruthenium anticancer complexes. *J. Med. Chem.* **2009**, *52*, 7753–7764.
(23) Stahl, S.; Werner, H. A new family of (arene)osmium(0) and (arene)osmium(II) complexes. *Organometallics* **1990**, *9*, 1876–1881.
(24) Peacock, A. F. A.; Habtemariam, A.; Fernandez, R.; Walland, V.; Fabbiani, F. P. A.; Parsons, S.; Aird, R. E.; Jodrell, D. I.; Sadler, P. J. Tuning the reactivity of osmium(II) and ruthenium(II) arene complexes under physiological conditions. *J. Am. Chem. Soc.* **2006**, *128*, 1739–1748.
(25) Wang, F.; Chen, H. M.; Parsons, S.; Oswald, L. D. H.; Davidson, J. E.; Sadler, P. J. Kinetics of aquation and anation of ruthenium-(II) arene anticancer complexes, acidity and X-ray structures of aqua adducts. *Chem.—Eur. J.* **2003**, *9*, 5810–5820.
(26) Kostrhunova, H.; Florian, J.; Novakova, O.; Peacock, A. F. A.; Sadler, P. J.; Brabec, V. DNA interactions of monofunctional organometallic osmium(II) antitumor complexes in cell-free media. *J. Med. Chem.* **2008**, *51*, 3635–3643.
(27) Barbieri, R. QSAR approach to understand the antitumor activity of organotins. *Inorg. Chim. Acta* **1992**, *191*, 253–259.
(28) Mendoza-Ferri, M.-G.; Hartinger, C. G.; Eichinger, R. E.; Stolyarova, N.; Severin, K.; Jakupec, M. A.; Nazarov, A. A.; Keppler, B. K. Influence of the spacer length on the in vitro anticancer activity of dinuclear ruthenium-arene compounds. *Organometallics* **2008**, *27*, 2405–2407.
(29) Song, R.; Park, S. Y.; Kim, Y.-S.; Kim, Y.; Kim, S.-J.; Ahn, B. T.; Sohn, Y. S. Synthesis and cytotoxicity of new platinum(IV) complexes of mixed carboxylates. *J. Inorg. Biochem.* **2003**, *96*, 339–345.
(30) Hall, M. D.; Amjadi, S.; Zhang, M.; Beale, P. J.; Hambley, T. W. The mechanism of action of platinum(IV) complexes in ovarian cancer cell lines. *J. Inorg. Biochem.* **2004**, *98*, 1614–1624.
(31) Oldfield, S. P.; Hall, M. D.; Platts, J. A calculation of lipophilicity of a large, diverse dataset of anticancer platinum complexes and the relation to cellular uptake. *J. Med. Chem.* **2007**, *50*, 5227–5237.
(32) Platts, J. A.; Hibbs, D. E.; Hambley, T. W.; Hall, M. D. Calculation of the hydrophobicity of platinum drugs. *J. Med. Chem.* **2001**, *44*, 472–474.
(33) Chen, H.; Parkinson, J. A.; Parsons, S.; Coxall, R. A.; Gould, R. O.; Sadler, P. J. Organometallic ruthenium(II) diamine anticancer complexes: arene-nucleobase stacking and stereospecific hydrogen-bonding in guanine adducts. *J. Am. Chem. Soc.* **2002**, *124*, 3064–3082.
(34) Aird, R. E.; Cummings, J.; Ritchie, A. A.; Muir, M.; Morris, R. E.; Chen, H.; Sadler, P. J.; Jodrell, D. I. In vitro and in vivo activity and cross resistance profiles of novel ruthenium (II) organometallic arene complexes in human ovarian cancer. *Br. J. Cancer* **2002**, *86*, 1652–1657.
(35) Eastman, A. Activation of programmed cell death by anticancer agents: cisplatin as a model system. *Cancer Cells* (*1989*) **1990**, *2*, 275–280.
(36) Jung, Y.; Lippard, S. J. Direct cellular responses to platinum-induced DNA damage. *Chem. Rev.* **2007**, *107*, 1387–1407.
(37) Yu, F.; Megyesi, J.; Price, P. M. Cytoplasmic initiation of cisplatin cytotoxicity. *Am. J. Physiol.* **2008**, *295*, F44–F52.
(38) Kerr, J. F.; Wyllie, A. H.; Currie, A. R. Apoptosis: a basic biological phenomenon with wide-ranging implications in tissue kinetics. *Br. J. Cancer* **1972**, *26*, 239–257.
(39) Gottlieb, E.; Armour, S. M.; Harris, M. H.; Thompson, C. B. Mitochondrial membrane potential regulates matrix configuration and cytochrome c release during apoptosis. *Cell Death Differ.* **2003**, *10*, 709–717.
(40) Kohler, H. R.; Dhein, J.; Alberti, G.; Krammer, P. H. Ultrastructural analysis of apoptosis induced by the monoclonal antibody anti-APO-1 on a lymphoblastoid B cell line. *Ultrastruct. Pathol.* **1990**, *14*, 513–518.
(41) Papadimitriou, J. C.; Drachenberg, C. B.; Shin, M. L.; Trump, B. F. Ultrastructural studies of complement mediated cell death: a biological reaction model to plasma membrane injury. *Virchows Arch.* **1994**, *424*, 677–685.
(42) Scorrano, L.; Ashiya, M.; Buttle, K.; Weiler, S.; Oakes, S. A.; Mannella, C. A.; Korsmeyer, S. J. A distinct pathway remodels mitochondrial cristae and mobilizes cytochrome c during apoptosis. *Dev. Cell* **2002**, *2*, 55–67.
(43) Yasugi, E.; Uemura, I.; Kumagai, T.; Nishikawa, Y.; Yasugi, S.; Yuo, A. Disruption of mitochondria is an early event during dolichyl monophosphate-induced apoptosis in U937 cells. *Zool. Sci.* **2002**, *19*, 7–13.
(44) Bindoli, A.; Rigobello, M. P.; Scutari, G.; Gabbiani, C.; Casini, A.; Messori, L. Thioredoxin reductase: a target for gold compounds acting as potential anticancer drugs. *Coord. Chem. Rev.* **2009**, *253*, 1692–1707.
(45) Chatterjee, S.; Kundu, S.; Bhattacharyya, A.; Hartinger, C. G.; Dyson, P. J. The ruthenium(II)-arene compound RAPTA-C induces apoptosis in EAC cells through mitochondrial and p53-JNK pathways. *J. Biol. Inorg. Chem.* **2008**, *13*, 1149–1155.
(46) Peacock, A. F. A.; Habtemariam, A.; Moggach, S. A.; Prescimone, A.; Parsons, S.; Sadler, P. J. Chloro half-sandwich osmium(II) complexes: influence of chelated N,N-ligands on hydrolysis, guanine binding, and cytotoxicity. *Inorg. Chem.* **2007**, *46*, 4049–4059.
(47) Peacock, A. F. A.; Melchart, M.; Deeth, R. J.; Habtemariam, A.; Parsons, S.; Sadler, P. J. Osmium(II) and ruthenium(II) arene maltolato complexes: rapid hydrolysis and nucleobase binding. *Chem.—Eur. J.* **2007**, *13*, 2601–2613.
(48) Morris, R. E.; Aird, R. E.; Murdoch, P. D.; Chen, H. M.; Cummings, J.; Hughes, N. D.; Parsons, S.; Parkin, A.; Boyd, G.; Jodrell, D. I.; Sadler, P. J. Inhibition of cancer cell growth by ruthenium(II) arene complexes. *J. Med. Chem.* **2001**, *44*, 3616–3621.
(49) Fernandez, R.; Melchart, M.; Habtemariam, A.; Parsons, S.; Sadler, P. L. Use of chelating ligands to tune the reactive site of half-sandwich ruthenium(II)-arene anticancer complexes. *Chem.—Eur. J.* **2004**, *10*, 5173–5179.
(50) Skehan, P.; Storeng, R.; Scudiero, D.; Monks, A.; McMahon, J.; Vistica, D.; Warren, J. T.; Bokesch, H.; Kenney, S.; Boyd, M. R. New colorimetric cytotoxicity assay for anticancer-drug screening. *J. Natl. Cancer Inst.* **1990**, *82*, 1107–1112.